

Studies of Laser-Driven 5 TeV e^+e^- Colliders in Strong Quantum Beamstrahlung Regime

M. Xie¹, T. Tajima², K. Yokoya³
and S. Chattopadhyay¹

¹*Lawrence Berkeley National Laboratory, USA*

²*University of Texas at Austin, USA*

³*KEK, Japan*

Abstract.

We explore the multidimensional space of beam parameters, looking for preferred regions of operation for a e^+e^- linear collider at 5 TeV center of mass energy. Due to several major constraints such a collider is pushed into certain regime of high beamstrahlung parameter, Υ , where beamstrahlung can be suppressed by quantum effect. The collider performance at high Υ regime is examined with IP simulations using the code CAIN. Given the required beam parameters we then discuss the feasibility of laser-driven accelerations. In particular, we will discuss the capabilities of laser wakefield acceleration and comment on the difficulties and uncertainties associated with the approach. It is hoped that such an exercise will offer valuable guidelines for and insights into the current development of advanced accelerator technologies oriented towards future collider applications.

INTRODUCTION

It is believed that a linear collider at around 1 TeV center of mass energy can be built more or less with existing technologies. But it is practically impossible to go much beyond that energy without employing a new, yet largely unknown method of acceleration. However, apart from knowing the details of the future technologies, certain collider constraints on electron and positron beam parameters are considered to be quite general and have to be satisfied, e.g. available wall plug power and the constraints imposed by collision processes: beamstrahlung, disruption, backgrounds, etc. Therefore it is appropriate to explore and chart out the preferred region in parameter space based on these constraints, and with that hopefully to offer valuable guide-

lines for and insights into the current development of advanced accelerator technologies oriented towards future collider applications.

Taking such a point of view, we examine collider performance at the final interaction point (IP) of a e^+e^- collider over a large space of beam parameters. We show that it becomes increasingly necessary at higher energy to operate colliders in high Υ regime and use to our advantage the quantum effect to suppress beamstrahlung. Although the quantum suppression effect was known and studied before with simple models [1-4], it has not been checked with full-blown simulation at high Υ regime that we are considering in this paper. As will be shown later, there are indeed several surprising features revealed by our simulations, in particular in the differential luminosity spectrum, which is a crucial factor for colliders.

Given beam parameters that are confirmed by simulation to be within acceptable level of beamstrahlung, we then discuss its implications for laser-driven acceleration. In particular we examine general characteristics and capabilities of laser wakefield acceleration and comment on the difficulties and uncertainties associated with the approach.

COLLIDER CONSIDERATIONS

In this section we will first discuss major collider requirements and constraints and organize the beam parameters in a way more convenient for exploration. We then scan the parameter space to find optimal regime of operation, and discuss its characteristics, as well as design options and trade-offs. These optimal designs are shown to be in high Υ regime. The collider performance at high Υ regime is examined with CAIN [5] simulations.

IP Requirements

The primary drive for developing ever more advanced accelerators is to expand both energy and luminosity frontiers for high energy physics applications. An important collider performance parameter is the geometrical luminosity given by $\mathcal{L}_g = f_c N^2 / 4\pi\sigma_x\sigma_y$ where f_c is the collision frequency, N is the number of particles per bunch, σ_x and σ_y are, respectively, the horizontal and vertical rms beam sizes at the IP. The real luminosity, however, depends on various dynamic processes at collision. Among them the most important ones are beamstrahlung and disruption [6]. These two processes are characterized by the beamstrahlung parameter $\Upsilon = 5r_e^2\gamma N / 6\alpha\sigma_z(\sigma_x + \sigma_y)$, and the disruption parameter $D_y = 2r_e N\sigma_z / \gamma\sigma_y(\sigma_x + \sigma_y)$, where γ is the Lorentz factor, r_e the classical electron radius, α the fine structure constant, and σ_z the rms bunch length. Beamstrahlung is in classical regime if $\Upsilon \ll 1$, and strong quantum regime if $\Upsilon \gg 1$. The physical effect of beamstrahlung is not directly reflected in the magnitude of Υ , but rather it is

more conveniently monitored through the average number of emitted photons per electron $n_\gamma = 2.54(\alpha\sigma_z\Upsilon/\lambda_c\gamma)U_0(\Upsilon)$ and relative electron energy loss $\delta_E = 1.24(\alpha\sigma_z\Upsilon/\lambda_c\gamma)\Upsilon U_1(\Upsilon)$. where $\lambda_c = \hbar/mc$ is the Compton wavelength, $U_0(\Upsilon) \approx 1/(1 + \Upsilon^{2/3})^{1/2}$, and $U_1(\Upsilon) \approx 1/(1 + (1.5\Upsilon)^{2/3})^2$.

So far we have given the major constraints imposed at the collision, which require n_γ and δ_E not be too large to cause luminosity degradation. Generally speaking, when these requirements are satisfied, other deteriorating effects such as pair creation and hadronic background will also be small [6]. Another major constraint for collider design is the available wall plug power which limits the beam power, given accelerator efficiency. We define the average power of both colliding beams $P_b = 2E_b N f_c$, the center of mass energy $E_{cm} = 2E_b$, and the beam energy $E_b = \gamma mc^2$.

It is noted from all the formulas given above that there are only six independent parameters and they are chosen for convenience to be $\{E_{cm}, \mathcal{L}_g, P_b, R, N, \sigma_z\}$, where R is the aspect ratio σ_x/σ_y . For collider design considerations we are interested in monitoring six quantities $\{f_c, \sigma_y, \Upsilon, D_y, n_\gamma, \delta_E\}$, and they are expressed in terms of the six independent parameters as follows

$$f_c = \left(\frac{P_b}{E_{cm}}\right) \left(\frac{1}{N}\right) \quad (1)$$

$$\sigma_y = \left(\frac{1}{\sqrt{4\pi}}\right) \left(\frac{1}{\sqrt{R}}\right) \left(\sqrt{\frac{P_b}{E_{cm}\mathcal{L}_g}}\right) (\sqrt{N}) \quad (2)$$

$$\Upsilon = \left(\frac{5\sqrt{\pi}r_e^2}{6\alpha mc^2}\right) \left(\frac{\sqrt{R}}{1+R}\right) \left(\sqrt{\frac{E_{cm}^3\mathcal{L}_g}{P_b}}\right) \left(\frac{\sqrt{N}}{\sigma_z}\right) \quad (3)$$

$$D_y = (16\pi mc^2 r_e) \left(\frac{R}{1+R}\right) \left(\frac{\mathcal{L}_g}{P_b}\right) (\sigma_z) \quad (4)$$

$$n_\gamma = 2.54U_0(\Upsilon)F, \quad \delta_E = 1.24\Upsilon U_1(\Upsilon)F \quad (5)$$

$$F = \left(\frac{5\sqrt{\pi}r_e^2}{3\lambda_c}\right) \left(\frac{\sqrt{R}}{1+R}\right) \left(\sqrt{\frac{E_{cm}\mathcal{L}_g}{P_b}}\right) (\sqrt{N}). \quad (6)$$

The advantage of organizing the independent and dependent parameters in such a way lies in its convenience for design optimization in the multidimensional parameter space, since in most situations many of the independent parameters can be fixed. For example, in this paper, we set $E_{cm} = 5\text{TeV}$

and $\mathcal{L}_g = 10^{35} \text{cm}^{-2} \text{s}^{-1}$ as our goal in energy and luminosity frontiers. For laser-driven acceleration, we assume $R = 1$ for reasons that will be explained later in this section. Furthermore, given maximum wall plug power, it is often adequate to consider P_b at a few discrete values corresponding to different accelerator efficiencies. Then for each fixed value of P_b we are left with only two independent parameters $\{N, \sigma_z\}$ to vary, and all the dependent parameters can thus be conveniently visualized in a surface or contour plot, as will be shown in the next section.

The design approach given here can be extended to integrate more collider parameters and the associated boundary conditions into the process of constrained optimization. For example, the beam size σ_y is related to two other important parameters: the normalized rms emittance ϵ_y and the betafunction at IP β_y by $\sigma_y = \sqrt{\beta_y \epsilon_y / \gamma}$. Once σ_y is determined, ϵ_y and β_y can be chosen according to other constraints, and vice versa. One constraint that is of immediate importance for the IP is the Oide limit [7], which sets the minimum achievable beam size: $\sigma_{min}[\text{m}] = 1.7 \times 10^{-4} \epsilon_y[\text{m}]^{5/7}$. Here we have used in the Oide limit a smaller numerical factor proposed by Irwin [8]. For later use, we define $F_{oide} = \sigma_y / \sigma_{min}$, the Oide limit is violated if $F_{oide} < 1$.

Before going to the exploration of parameter space using Eqs.(1-6), it is instructive to look at the more transparent scaling laws in two dimensional parameter space $\{N, \sigma_z\}$ when $\{E_{cm}, \mathcal{L}_g, P_b, R\}$ are considered fixed

$$f_c \sim 1/N, \quad \sigma_y \sim \sqrt{N}, \quad D_y \sim \sigma_z, \quad \Upsilon \sim \sqrt{N}/\sigma_z \quad (7)$$

$$n_\gamma \sim U_0(\Upsilon)\sqrt{N}, \quad \delta_E \sim \Upsilon U_1(\Upsilon)\sqrt{N}. \quad (8)$$

In the limit $\Upsilon \gg 1$, $U_0(\Upsilon) \rightarrow 1/\Upsilon^{1/3}$, $\Upsilon U_1(\Upsilon) \rightarrow 1/\Upsilon^{1/3}$. Eq.(8) becomes

$$n_\gamma \sim (N\sigma_z)^{1/3}, \quad \delta_E \sim (N\sigma_z)^{1/3}. \quad (9)$$

We see from Eqs.(7,9) that once in the high Υ regime there are two approaches to reduce the effects of beamstrahlung: either by reducing N or by reducing σ_z . The consequences on the collider design and the implied restrictions on the approaches, however, can be quite different. Reducing N requires f_c to be increased and σ_y decreased, thus the approach is limited by the constraints on f_c and σ_y . Reducing σ_z , on the other hand, is not directly restricted in this regard. Also the dependencies of Υ on the two approaches are quite the opposite. The second approach clearly demonstrates the case that beamstrahlung can indeed be suppressed by having larger Υ .

We now come to explain why it is reasonable to assume round beam $R = 1$. The current designs of linear colliders at 0.5 TeV are all based on damping ring technology which provides much smaller emittance in the vertical dimension. Taking advantage of this feature, beam distribution at the IP has been made

very flat, $R \gg 1$, to suppress beamstrahlung. However, first of all, it is not clear at this point what would be the injector of choice for future laser-driven accelerator, if emittances can be made as asymmetrical as in the damping ring, or if possible, would it be compatible with, for example, transverse focusing channel of the acceleration scheme. Secondly, as will be shown in the next section for round beam, the required beam size is already in the Å level. A flat beam requires the beam size in one dimension be made even smaller, thus pushing the limit for tight beam positioning control. Nonetheless, one should keep in mind that making $R \gg 1$ is still a knob for further suppression of beamstrahlung, even in strong quantum regime as can be seen from Eqs.(1-6).

Parameter Optimization

Using the formulas provided in the previous section: Eqs.(1-6), we are now ready to explore the parameter space. As mentioned before we will consider the situation with $\{E_{cm} = 5\text{TeV}, \mathcal{L}_g = 10^{35}\text{cm}^{-2}\text{s}^{-1}, R = 1\}$. Assuming wall plug power for such a collider is limited to 2 GW [8], and the overall "wall plug to beam" efficiency is within the range of 0.1% to 10%, we will look at three cases with P_b being 2 MW, 20 MW and 200MW, respectively.

Figure 1 shows the contour plots of parametric scans for the cases with $P_b = 2\text{MW}$ (left column) and 20MW (right column). Due to page limitation, we show only a few out of many quantities that can be monitored in $\{N(10^8), \sigma_z(\mu\text{m})\}$ space, they are, starting from the top row: n_γ , Υ and $\sigma_y(\text{nm})$. From these scans one may choose optimal operation point $\{N, \sigma_z\}$ based on various constraints imposed on the independent as well as dependent quantities. Using the plots in the bottom row one can also determine $\epsilon_y(\text{nm})$ and $\beta_y(\mu\text{m})$ at different values of σ_y , and from there to check F_{oide} . The type of parametric scans shown here are used as a guide to pick specific parameter sets given in Table 1 for three values of beam power. Several performance parameters computed from the formulas are given in Table 2, some of them can be directly compared with simulations. It is noted here we have chosen to make n_γ significantly less than 1 and same for all three cases, and violate the Oide limit by about 10% on purpose to relax other parameters.

High Υ IP Simulation

Although the simple formula, Eq.(5), takes into account strong quantum beamstrahlung with high Υ , some important effects are nonetheless neglected, for example, disruption and multiphoton processes [6]. It is therefore necessary to examine its predictions with full-blown simulations. We use a Monte-Carlo simulation code recently developed by Yokoya [5] to study QED processes at the IP for e^+e^- and $\gamma\gamma$ colliders. This code is a superset of the well-known code ABEL by the same author. Care has been taken to ensure that there is

enough resolution in the simulation at such high Υ values to yield reliable QED prediction. This is established by verifying that results changes insignificantly by changes of resolution grids.

Figure 2 gives the differential e^+e^- luminosities for the case I, II, III in Table 1. It is noted that the luminosity spectrum is characterized by an outstanding core at the full energy and a very broad, nearly flat halo. One see from Table 3, taking case II for example, although on average the beam loses 26% of its energy and has a rms energy spread of 36%, the core itself within 1% of full energy still accounts for 65% of the geometrical luminosity. The outstanding core is more than two orders of magnitude above the halo. The sharpness and the high luminosity of the core is rather surprising but pleasantly so. Comparing simulation results in Table 3 for n_γ and δ_E with that calculated from the formulas in Table 2, one see the agreement varies from being reasonably good at lower Υ to rather poor at higher Υ . It seems to indicate that the formulas can be used only as a rough guideline for collider design at high Υ . It is interesting to note that the core luminosity is somewhat larger for the case with higher beamstrahlung loss, which is probably due to disruption enhancement as indicated by the larger value of D_y in Table 2.

Another major deteriorating process at high Υ is coherent pair creation. The number of pairs created per primary electron, n_p , is given in Table 2 by formulas [6] and in Table 3 by simulations. According to our simulations the incoherent pair creation is 2 to 3 orders of magnitude smaller than that of the coherent pairs, thus negligible. Finally we point out that such a differential luminosity spectrum should be rigorously assessed together with the background of beamstrahlung photons and coherent pairs from the point of view of particle physics and detector considerations. Only then, one may judge if operation of colliders at high Υ regime is indeed a viable approach for high energy physics applications.

ACCELERATOR CONSIDERATIONS

As seen from Eq.(9), an effective way to suppress beamstrahlung is to reduce σ_z , which naturally favors laser acceleration as it offers much shorter acceleration wavelength than that of conventional microwaves. For laser wakefield acceleration, typical wavelength of accelerating wakefield is $\sim 100 \mu\text{m}$, which is in the right range for the required bunch length in Table 1. Laser wakefield acceleration [9,10] has been an active area of research in recent years primarily due to the major technological advance in short pulse TW lasers [11]. The most recent experiment at RAL has demonstrated an acceleration gradient of 100 GV/m and produced beam-like properties with 10^7 accelerated electrons at $40\text{MeV} \pm 10\%$ and a normalized emittance of $\epsilon < 5\pi \text{ mm-mrad}$ [12].

For beam parameters similar to that in Table 1, we consider a laser wakefield accelerator system consisting of multiple stages with a gradient of 10 GeV/m.

With a plasma density of 10^{17}cm^{-3} , such a gradient can be produced in the linear regime with more or less existing T³ laser, giving a plasma dephasing length of about 1 m [13]. If we assume a plasma channel tens of μm in width can be formed at a length equals to the dephasing length, we would have a 10 GeV acceleration module with an active length of 1 m. Of course, creating and maintaining a plasma channel of the required quality is no simple matter. To date, propagation in a plasma channel over a distance of up to 70 Rayleigh lengths (about 2.2 cm) of moderately intense pulse ($\sim 10^{15}\text{W}/\text{cm}^2$) has been demonstrated [14]. New experiment aiming at propagating pulses with intensities on the order of $10^{18}\text{W}/\text{cm}^2$ (required for a gradient of 10 GeV/m) is underway [13].

Table 1. Beam Parameters at Three Values of Beam Power

CASE	$P_b(\text{MW})$	$N(10^8)$	$f_c(\text{kHz})$	$\varepsilon_y(\text{nm})$	$\beta_y(\mu\text{m})$	$\sigma_y(\text{nm})$	$\sigma_z(\mu\text{m})$
I	2	0.5	50	2.2	22	0.1	0.32
II	20	1.6	156	25	62	0.56	1
III	200	6	416	310	188	3.5	2.8

Table 2. Results Given By the Formulas

CASE	Υ	D_y	F_{oide}	n_γ	δ_E	n_p	$\mathcal{L}_g(10^{35}\text{cm}^{-2}\text{s}^{-1})$
I	3485	0.93	0.89	0.72	0.2	0.19	1
II	631	0.29	0.89	0.72	0.2	0.12	1
III	138	0.081	0.91	0.72	0.2	0.072	1

Table 3. Results Given By CAIN Simulations

CASE	n_γ	δ_E	σ_e/E_0	n_p	$\mathcal{L}/\mathcal{L}_g(W_{\text{cm}} \in 1\%)$	$\mathcal{L}/\mathcal{L}_g(W_{\text{cm}} \in 10\%)$
I	1.9	0.38	0.42	0.28	0.83	1.1
II	0.97	0.26	0.36	0.12	0.65	0.80
III	0.84	0.21	0.32	0.06	0.62	0.75

Although a state-of-the-art T³ laser, capable of generating sub-ps pulses with 10s of TW peak power and a few Js of energy per pulse [11], could almost serve the need for the required acceleration, the average power or the rep rate of a single unit is still quite low, and wall-plug efficiency inadequate. In addition, injection scheme and synchronization of laser and electron pulse from

stage-to-stage to good accuracy have to be worked out. Yet another important consideration is how to generate and maintain the small beam emittance in the transverse focusing channel provided by plasma wakefield throughout the accelerator leading to the final focus. There are various sources causing emittance growth, multiple scattering [15], plasma fluctuations [16] and mismatching between acceleration stages, to name just a few. Should the issues of guiding, staging, controllability, emittance preservation, etc. be worked out, there is hope that wakefields excited in plasmas will have the necessary characteristics for particle acceleration to ultrahigh energies.

CONCLUSIONS

We have explored the possibilities of operating a 5 TeV linear collider in the strong quantum beamstrahlung regime. To take the full advantage of quantum suppression of beamstrahlung, we have searched a large space of multidimensional collider parameters for the preferred regime of operation. By making collider scaling laws transparent, we found that reducing bunch length is an effective approach to suppress beamstrahlung, which naturally favors laser-driven acceleration. The prediction of scaling laws has been checked with full-blown IP simulations, and the results are quite encouraging. We have discussed the implied requirements for laser wakefield acceleration. The parameters of a 10 GeV module in a 5 TeV collider vision demonstrates both encouraging and sobering features that calls for further developments and innovations.

REFERENCES

1. Himel T., Siegrist J., AIP Conf. Proc., **130**, 602 (1985).
2. Chen P., Yokoya K., *Phys. Rev. Lett.*, **61**, 1101 (1988).
3. Blankenbecler R., Drell S., *Phys. Rev. D*, **37**, 3308 (1988).
4. Jacob M., Wu T. T., *Nucl. Phys.*, **B318**, 53 (1989).
5. For code and manual, see <http://jlcux1.kek.jp/subg/ir/Program-e.html>.
6. Yokoya K., Chen P., *Frontiers of Particle Beams*, **400**, 415 (1992).
7. Oide K., *Phys. Rev. Lett.*, **61**, 1713 (1988).
8. Irwin J., AIP Conf. Proc., **335**, 3 (1995).
9. Tajima T., Dawson J., *Phys. Rev. Lett.*, **43**, 267 (1979).
10. For recent experiment see Nakajima K., et. al., these proceedings.
11. For a review, see Downer M. C., Siders C. W., these proceedings.
12. For reference see Chattopadhyay S., et. al., Snowmass'96, LBL-39655, (1996).
13. Leemans W. P., et.al., *IEEE Trans. on Plasma Science*, **24**, 331 (1996).
14. Durfee III C. G., Milchberg H. M., *Phys Rev. Lett.* **71**, 2409 (1993).
15. Montague B. W., Schnell W., AIP Conf. Proc., **130**, 146 (1985).
16. Horton W., Tajima T., et.al., *Phys. Rev. A*, **31**, 3937 (1985).

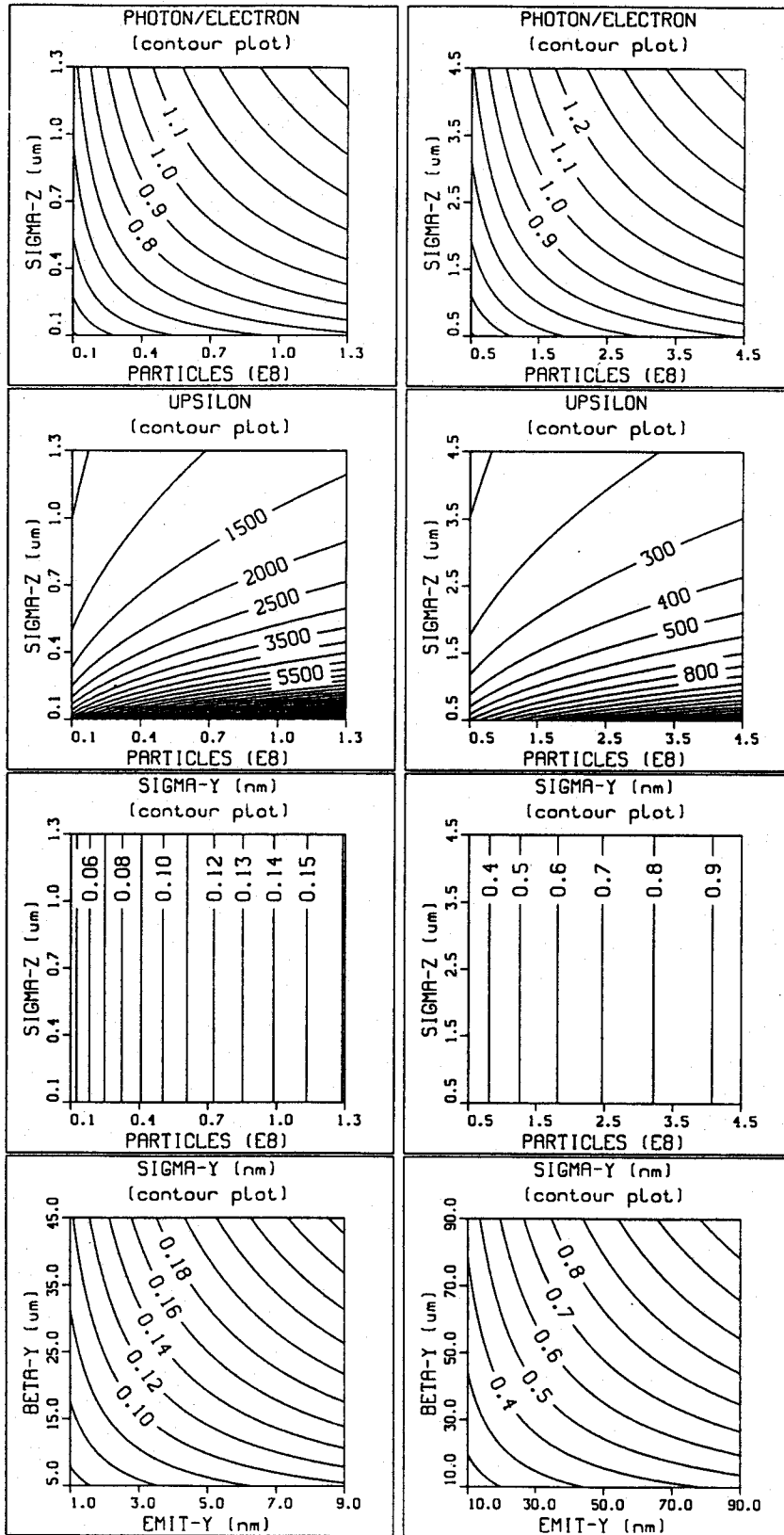


FIGURE 1. Parameter scans for $P_b = 2\text{MW}$ (column 1) and 20MW (column 2).

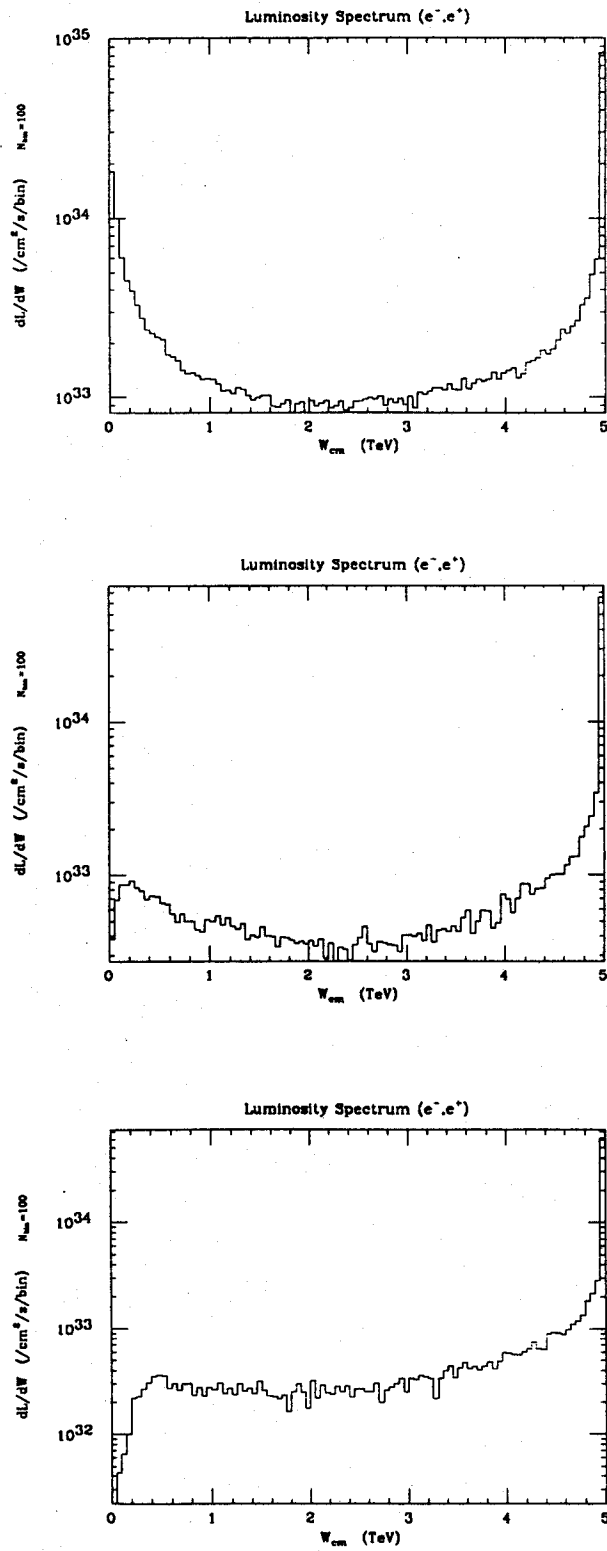


FIGURE 2. e^+e^- luminosity spectrum for case I (top), II (middle), III (bottom).